Research Article | Vol. 27, No. 10 | 13 May 2019 | OPTICS EXPRESS 14657
Optics EXPRESS

# Spatially-targeted laser fabrication of multi-metal microstructures inside a hydrogel

MANAN MACHIDA,[1] TAKURO NIIDOME,[2] HIROAKI ONOE,[1,3] ALEXANDER HEISTERKAMP,[1,4,5] AND MITSUHIRO TERAKAWA[1,6,*]

[1]*School of Integrated Design Engineering, Keio University, 3-14-1, Hiyoshi, Kohoku-ku, Yokohama 223-8522, Japan*
[2]*Faculty of Advanced Science and Technology, Kumamoto University, 2-39-1 Kurokami, Chuo-ku, Kumamoto 860-8555, Japan*
[3]*Department of Mechanical Engineering, Keio University, 3-14-1, Hiyoshi, Kohoku-ku, Yokohama 223-8522, Japan*
[4]*Institut fuer Quantenoptik, Gottfried Wilhelm Leibniz University Hannover, Am Welfengarten 1, 30167 Hannover, Germany*
[5]*Industrial and Biomedical Optics Department, Laser Zentrum Hannover e.V., Hollerithallee 8, D-30419 Hannover, Germany*
[6]*Department of Electronics and Electrical Engineering, Keio University, 3-14-1, Hiyoshi, Kohoku-ku, Yokohama 223-8522, Japan*
**terakawa@elec.keio.ac.jp*

**Abstract:** The spatially-targeted fabrication of bimetallic microstructures coexisting in the supporting hydrogel is demonstrated by multi-photon photoreduction. Microstructures composed of gold and silver were fabricated along a predefined trajectory by taking advantages of the hydrogel's ionic permeability. Different resonant wavelengths of optical absorption were obtained for gold, silver, and their bimetallic structures. Transmission electron microscopy and energy dispersive X-ray analysis revealed that the optical properties are attributable to the formation of bimetallic structure consisted of core–shell nanoparticles. The fabrication of dissimilar metal structures within hydrogel is a promising technique for optically driven actuators in soft robotics and sensing applications by allowing for site-selective optical properties.



## 1. Introduction

Metal micro- and nanostructures exhibit unique optical properties depending on the size, shape, and material of the structures, which enables a wide range of applications including optical sensing [1] and biological analysis [2,3]. Color hologram [4] and surface-enhanced Raman scattering (SERS) sensors [5] have also been studied by taking advantage of the wavelength-selective optical absorption of metal nanoparticles or nanorods, whose property depends on their diameter or aspect ratio. The applicability of metal micro- and nanostructures will be further expanded through the combination of multiple dissimilar metals, because bimetallic structures, which by definition are composed of two different metal elements, show attractive properties dependent on the size, compound ratio and morphology of the structures [6]. In one technique for fabricating bimetallic nanostructures, gold core–silver shell nanoparticles were fabricated by reduction of silver ions around gold nanoparticles in water [7]. Gold/silver alloy nanoparticles have also been formed by laser-melted gold and silver nanostructures [8]. The site-selective optical properties can be realized by forming bimetallic structures at arbitrary sites on or inside a substrate or in a supporting base material. For example, Tien et al. reported the fabrication of gold and silver aligned microstructures on a glass substrate by using a multistep process of soft-lithography, etching, and metal evaporation [9]. Two-dimensional (2D) gold and aluminum complex structures in a substrate [10] and aluminum/ITO nanogap structures on a poly(ethylene terephthalate) (PET)

#362736 https://doi.org/10.1364/OE.27.014657
Journal © 2019 Received 19 Mar 2019; revised 17 Apr 2019; accepted 30 Apr 2019; published 6 May 2019

Optics EXPRESS

substrate were fabricated by adhesion lithography for novel applications in flexible devices [11]. Nevertheless, a fabrication technique for bimetallic structures that is applicable to an arbitrary three-dimensional (3D) space would enable various optical applications including optically-driven actuators, photonic crystals, and metamaterials.

Femtosecond laser direct writing via multi-photon processing has emerged as a powerful 3D fabrication technique for micro- and nanostructures. Photopolymerization or photoreduction occur with a high degree of spatial accuracy by multi-photon absorption in the tightly focused space of the laser pulses. Such 3D structures can be fabricated with submicron to multi-micron resolution by adjusting the position of the focal point. Because the fabrication of 3D polymer structures was demonstrated in 1997 [12], many studies have reported on the fabrication of polymer structures based on multi-photon photopolymerization [13–15]; beyond this, the fabrication of a multi-polymer structure was demonstrated recently [16]. A few papers have also reported the selective metallization of polymer microstructures that were formed via multi-photon photopolymerization. In 2007, LaFratta et al. fabricated 2D metal microstructures by electroless deposition of copper on the selective-functionalized surface of the acrylic structures [17]. Takeyasu et al. demonstrated the fabrication of 3D silver/polymer conjugated microstructures by site-selective metal deposition on photopolymer structures [18]. Although these methods require multiple complex steps for the fabrication, they can provide site-selective fabrication of metal and polymer multi-structures. The fabrication of 2D [19–21] or 3D [22,23] metal microstructures on a glass substrate by multi-photon photoreduction has been demonstrated by focusing femtosecond laser pulses into a metal ion solution or into a polymer material. In these studies, the liquid solution or polymer matrix needed to be removed after fabricating the metal microstructures. Recently, the fabrication of metal microstructures inside a supporting base material containing metal ions was demonstrated [24–26]. Metal nanostructures were also fabricated inside glass by laser irradiation of gold- or silver-doped glass substrate [27,28]. With such methods, the fabrication of arbitrary multi-metal structures is difficult because the metal ions must be doped or mixed into a supporting material in advance before the laser irradiation.

Hydrogel, which is a 3D polymer material containing water, is a promising supporting material for metal structures for the realization of novel optical, mechanical, and biomedical devices owing to the good biocompatibility and flexibility [29,30]. Kang et al. reported their pioneering study on the fabrication of silver nanodots in gelatin by multi-photon photoreduction, in which silver ions were provided by mixing in silver nitrate before the cross-linking of the gelatin [26]. Shortly thereafter, we fabricated silver line structures inside poly(ethylene glycol) diacrylate (PEGDA) hydrogel—a typical synthetic polymer hydrogel—by multi-photon photoreduction [31,32]. Various applications including optically driven actuators that enable much complex movement as well as wavelength-selective optical sensors would be realized if dissimilar metal structures are able to be fabricated spatial selectively within hydrogel.

In this paper, we demonstrate—for the first time, to the best of our knowledge—the spatially-targeted fabrication of multi-metal structures coexisting in the same supporting hydrogel by multi-photon photoreduction. We took advantage of the hydrogel's permeability to fluids, i.e., we added metal ions alternately by immersing the hydrogels into respective metal ion solutions after photo–cross-linking. The optical absorbance properties of the fabricated bimetallic structures exhibit a tunable wavelength of absorption, which is attributable to the plasmonic resonance of nanostructures as verified by electron microscopy results.

## 2. Materials and methods

PEGDA (average molecular mass: 6000) and the photoinitiator Irgacure2959 were purchased from Sigma-Aldrich Co. LLC (St. Louis, MO). PEGDA (0.1 g) was dissolved in 1 ml of pure water containing 1% photoinitiator and stirred for 15 min. The solution was placed in a mold

and illuminated by a 365 nm light from a UV lamp (6W) for 20 min to induce photo–cross-linking. The hydrogel of 5 mm in length, 3 mm in width, and 3 mm in thickness was used for the experiments of the optical microscope observation of the fabricated metal microstructures, while the disk-shaped hydrogel 12 mm in diameter and 1 mm in thickness was used for the optical property measurements. The cross-linked hydrogel was stored in pure water overnight. For fabrication of single metal microstructures (i.e., gold or silver), the hydrogel was immersed in gold(III) chloride (Sigma-Aldrich Co. LLC) solution (0.4 mg/ml) or silver nitrate (Sigma-Aldrich Co. LLC) solution (40 mg/ml) for 10 min to add gold or silver ions, respectively; then, femtosecond laser pulses were focused. For fabrication of gold and silver bimetallic microstructures, we used a procedure that took advantage of hydrogel's ionic permeability. Gold structures were fabricated by femtosecond laser irradiation of the hydrogel containing gold(III) chloride solution (0.4 mg/ml); subsequently, the hydrogel was immersed in pure water overnight to remove residual gold ions. The hydrogel was then immersed in silver nitrate solution (40 mg/ml) for 10 min prior to another scanning of femtosecond laser pulses to form the silver structures coexisting with the preformed gold structures in the same hydrogel.

Femtosecond laser pulses with a wavelength of 522 nm at 63 MHz repetition rate, was used for the fabrication of gold and/or silver microstructures by multi-photon photoreduction of the metal ions. The pulse duration of the output pulse was 192 fs. An objective lens (numerical aperture (NA) 0.4, working distance 1.2 mm, Olympus; Tokyo, Japan) was used to focus the laser pulses for the fabrication of the grid formed by gold and/or silver, whereas a water immersion objective lens (NA 1.0, working distance 2.0 mm; Olympus) was used for fabrication when the two gratings crossed at different distances from the surface of the hydrogel. The metal microstructures were fabricated along a predefined trajectory by using a computer-controlled, three-axis encoded (XYZ) motorized stage.

The fabricated structures inside the wet hydrogel were observed with an inverted transmission optical microscope (Eclipse Ti-E, Nikon; Tokyo, Japan). The microscope images of the fabricated structures were obtained by a camera (DS-Ri1, Nikon) attached to the microscope. The hydrogel was dried and thinned using pestle and mortar, and then the thin film of 100 nm thickness was prepared by slicing the sample in an epoxy-molding compound. The slice was observed by transmission electron microscopy (TEM, Tecnai Spirit TEM, FEI; Hillsboro, Oregon). Elemental analysis of the fabricated line structure formed from gold and silver was performed by energy dispersive X-ray (EDX) spectroscopy during scanning TEM (STEM, Tecnai Osiris, FEI). The optical absorbance spectra of the hydrogel in which metal grids or gratings were fabricated were measured using a spectrometer (USB4000, Ocean Optics, Inc.; Largo, Florida).

## 3. Results and discussion

### *3.1 Fabrication of bimetallic structures*

Figure 1 shows a bright-field microscope image of the gold and silver microstructures fabricated in the PEGDA hydrogel, taken 250 μm from the surface of the hydrogel. Three microstructures with different sizes (structure widths of 140 μm, 93 μm, and 47 μm) were fabricated by raster scanning (Fig. 1(c)) according to the predefined model design (Figs. 1(a) and 1(b)). The characters of "Keio Univ" were formed by laser scanning the hydrogel containing gold ions. After the replacement of gold ions to silver ions, the nib (i.e., fountain pen tip)-shaped silver microstructures were fabricated by laser scanning with the presence of silver ions. The result clearly shows dissimilar metal microstructures that were fabricated in the same hydrogel by multi-photon photoreduction. The laser power during the fabrication was 15.0 mW (corresponding to 0.24 nJ per pulse). The scanning speed was 50 μm/s for the fabrication of the structures with widths of 140 μm and 93 μm, whereas the scanning speed was 100 μm/s for the fabrication of the microstructure with a width of 47 μm. Red and yellow colors were observed for the fabricated gold and silver microstructures, respectively, which

Optics EXPRESS

are attributable to the surface plasmon resonances (SPR) of the metal nanoparticles. The result indicates that the fabricated microstructures comprise metal nanoparticles. The black color in the center of characters is explainable by the higher density of gold nanoparticles.

Figure 2 shows bright-field microscope images of line structures formed from gold and/or silver. The line structures in which the gold line structures were fabricated first followed by silver structure fabrication (Fig. 2(b)) exhibit colors respective of those in Fig. 1, which shows the coexistence of gold and silver structures consisting of their respective nanoparticles in the same hydrogel. However, the silver line structures changed from yellow (Fig. 2(c)) to gray (horizontal lines in Fig. 2(d)) when gold ions were added to the hydrogel after the fabrication of the silver line structure. These results are explainable by galvanic replacement reactions between gold ions and silver metal, i.e., the oxidation of silver structures by the gold ions [33,34]. The gold ions reduced by laser scanning also formed gray line structures possibly due to the residual silver ion which was reduced simultaneously (vertical lines in Fig. 2(d)). On the contrary, the limited change of color in Fig. 2(b) is attributable to the removal of the gold ions from the hydrogel by water immersion after gold microstructure fabrication. The osmotic pressure difference, induced by the different ionic strengths and pH [35] between pure water and the hydrogel containing dissolved gold(III) chloride, might cause the removal of gold ions.

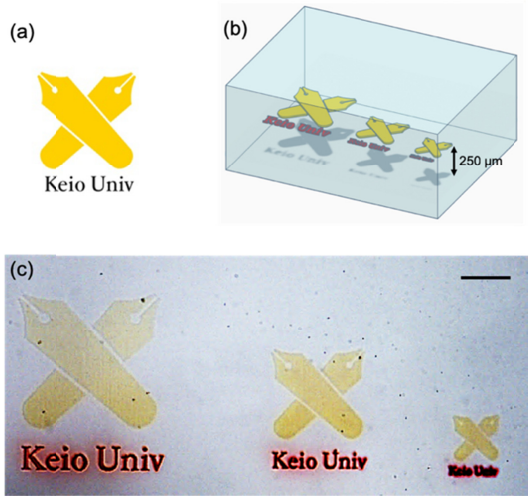


Fig. 1. Keio logo–shaped gold and silver microstructures fabricated inside a hydrogel. (a) Illustration and (b) computer-generated image of the predefined model design. (c) Bright-field microscope image of the fabricated microstructures inside a hydrogel showing the unaltered exhibiting color. The characters of "Keio Univ" and the nib-shaped microstructures were fabricated with gold and silver, respectively. The scale bar represents 50 μm.

Optics EXPRESS

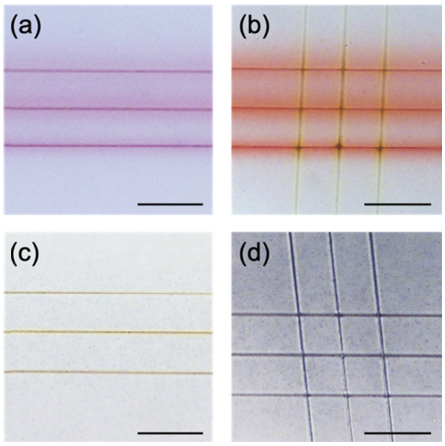


Fig. 2. Bright-field microscope images of line structures formed from gold and/or silver within a hydrogel. (a) Gold line structures. (b) Gold and silver line structures in which horizontal gold line structures were fabricated prior to the fabrication of vertical silver line microstructures. (c) Silver line structures. (d) Gold and silver line structures in which horizontal silver line structures were fabricated prior to the fabrication of vertical gold line structures. The scanning speed and laser power were 25 μm/s and 10.4 mW, respectively. The scale bars represent 50 μm.

Figure 3 shows bright-field microscope images of grids and one-dimensional (1D) gratings formed from gold and/or silver. The distance from the surface of the hydrogel to the structures was 250 μm. The pitch between adjacent lines of grating was 10 μm. Line structures exhibit different colors depending on the metals. The metal gratings (Figs. 3(a) and 3(b)) were lighter in color compared to the metal grids (Figs. 3(c) and 3(d)) consisting of the same metals. As seen in Fig. 2, the reduction of metal ions also occurs around the line structures. The difference in background colors in Figs. 2 and 3 is explainable by the distances of adjacent lines, i.e. line density. The vertical gold grating in the bimetallic grid (Fig. 3(e)) was fabricated prior to the horizontal silver grating to avoid the galvanic replacement reactions observed when gold structures were fabricated after silver structures. As shown in the inset of Fig. 3(e), the vertical and horizontal gratings have consistent different colors (red and yellow for the gold and silver structures, respectively); notably, intersection points are colored differently from the lines.

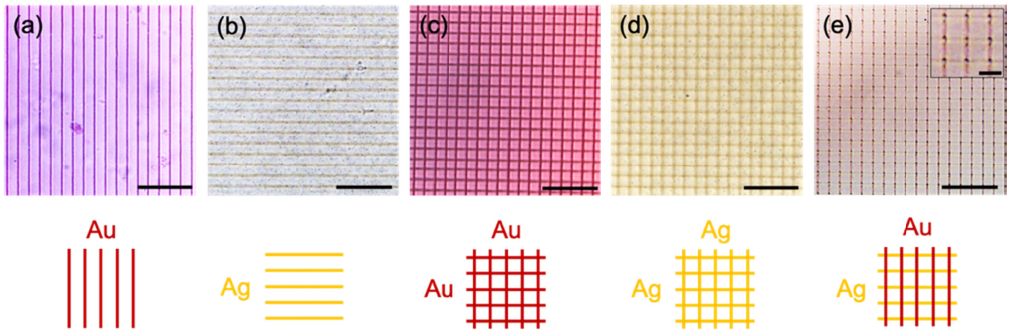


Fig. 3. Bright-field microscope images of fabricated gold or/and silver gratings and grids inside a hydrogel. (a) Gold and (b) silver gratings, (c) gold and (d) silver grids, and (e) combination grid of vertical gold grating and horizontal silver grating in which the gold line structures were fabricated first followed by silver structure fabrication. The scanning speed and laser power were 25 μm/s and 10.4 mW, respectively. The scale bars represent (a)–(e) 50 μm or (the inset of (e)) 10 μm.

Optics EXPRESS

### *3.2 Optical absorbance spectra*

The optical absorbance spectra of the fabricated grids and gratings formed from gold and/or silver within hydrogel were obtained (Fig. 4(a)). The absorbance peaks of the gold and silver gratings were observed at approximately 550 nm and 458 nm, respectively, which are consistent with the typical resonant wavelengths of gold and silver nanoparticles with diameters from 60 to 80 nm [36,37]. However, because the fabricated metal structures were embedded in a hydrogel matrix, it should be noted that the absorbance peaks could be shifted due to the binding to an organic structure [38]. The diameters of the fabricated nanoparticles are assumed to be smaller than 60 nm by considering the shift of the absorbance peak. The absorbance peaks of the gold and silver grids, fabricated by orthogonally-crossed gratings, exhibited red shifts of approximately 15 nm to 18 nm compared to the peaks of the respective metal gratings. The peak wavelengths of metal nanoparticles are well known to depend on the particle's size, showing a red-shift with increasing nanoparticle diameter [37]. The size distribution of the metal nanoparticles could be shifted, probably due to the duplicate scanning of femtosecond laser pulses, which might be significant at the intersection points during grid fabrication. The observed absorbance peak of the gold/silver bimetallic grid was 520 nm. It should be noted that the spectrum does not show double peaks—the typical spectrum for the mixture of two different materials—but a significant single peak that dominates gold and silver peaks. The result may suggest the formation of bimetallic nanostructures such as core–shell or alloy nanoparticles.

We attempted to shift the peak wavelength by changing the laser scanning speed of the femtosecond laser during the fabrication of bimetallic grids. The laser scanning speed for the fabrication of gold grating was fixed at 25 μm/s, whereas that for the subsequent silver grating was varied from 5 μm/s to 100 μm/s (Fig. 4(b) and enlarged image of peaks in Fig. 4(c)). The bimetallic grid with silver grating fabricated at 100 μm/s had an absorbance spectrum shifted to longer wavelengths, whereas the bimetallic grid with silver grating fabricated at 5 μm/s had an absorbance spectrum shifted to shorter wavelengths compared to the case at 25 μm/s. Different resonance wavelengths were obtained by controlling the quantity of reduced silver ions by changing the laser scanning speed, i.e., by changing the number of pulses overlapping for the fabrication of silver grating. The peak wavelength would also be controlled much precisely by changing the size of the fabricated nanoparticles, since the peak wavelength depends on the size of nanoparticles [39,40].

Gold and silver gratings crossing at different distances from the surface of the hydrogel were fabricated by changing the focal depth of the femtosecond laser pulses. First, the gold grating was fabricated at 250 μm from the surface of the hydrogel; then, the silver grating was fabricated at various distances closer to the surface. Figure 4(d) shows the absorbance spectra of such grating layers formed from gold and silver; an enlarged image of the peaks is shown in Fig. 4(e). The absorbance peak gradually showed a red-shift as the distance between the two grating layers was increased. The quantity of formed pure gold nanoparticles could have increased, as increasing the distance between two grating layers formed from gold and silver—and hence the resonance wavelength of the two grating layers—shifted the lower wavelength side of the absorbance peak, i.e., the side corresponding to the pure gold nanoparticles' spectrum. The result may also suggest that the quantity of formed bimetallic nanostructures, such as core–shell or alloy nanoparticles, decreased as the distance between two grating layers increased.

Optics EXPRESS

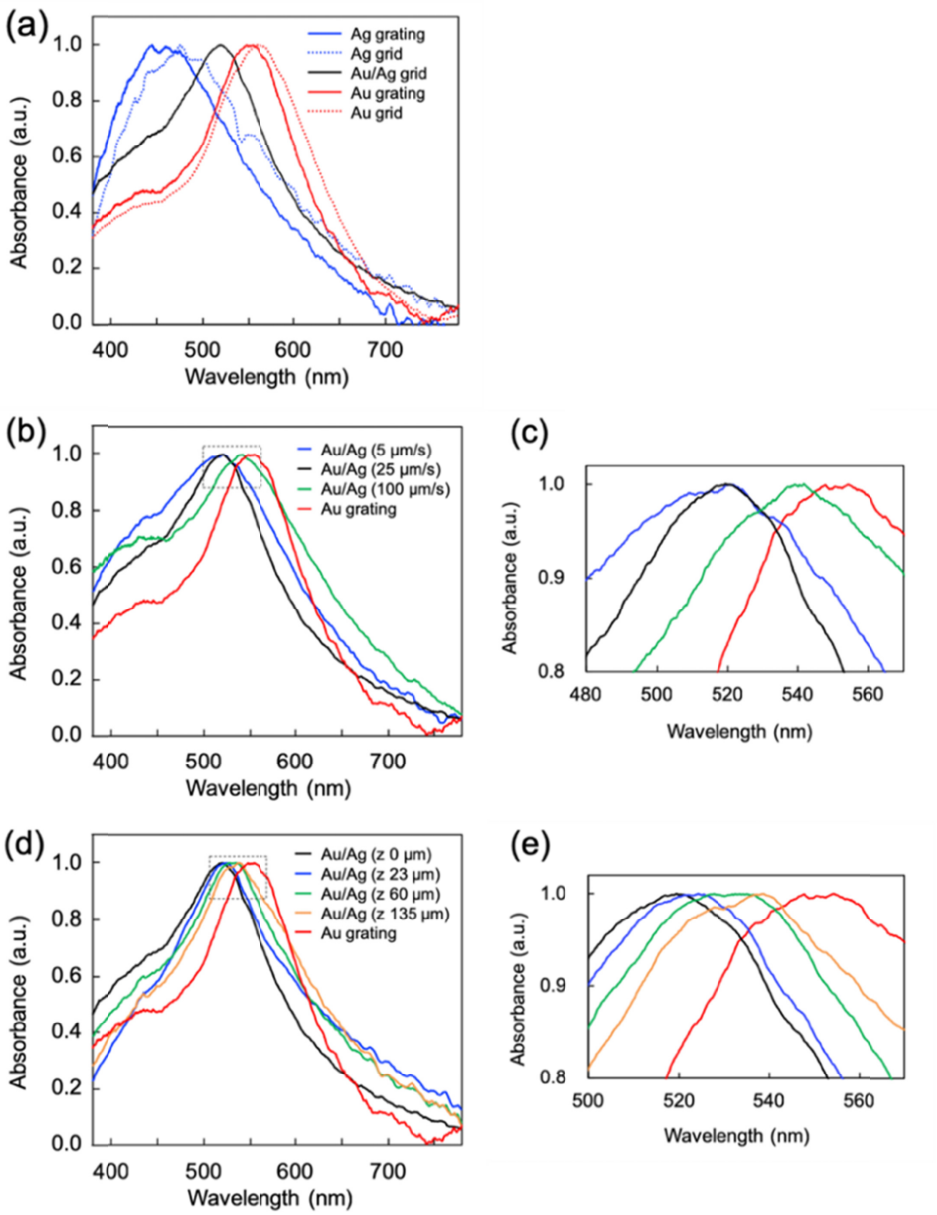


Fig. 4. Absorbance spectra of metal line structures fabricated inside a hydrogel. (a) Absorbance spectra of the gold or/and silver grids and gratings in a hydrogel. (b) Absorbance spectra of the gold/silver bimetallic grids with the laser scanning speed for the fabrication of gold grating fixed at 25 μm/s, whereas that for the silver grating was varied from 5 to 100 μm/s. (c) Enlarged image of peaks in (b). (d) Absorbance spectra of the fabricated gold/silver gratings crossing at different distances from the surface of a hydrogel: the distances between gold and silver gratings ($z$) were varied from 0 to 135 μm. (e) Enlarged image of peaks in (d).

### *3.3 Transmission electron microscopy (TEM) and energy dispersive X-ray (EDX) analysis*

To confirm the formation of bimetallic nanostructures, we performed scanning TEM (STEM) and EDX analysis on the fabricated bimetallic line structures formed from gold and silver

Optics EXPRESS

(Fig. 5). Nanoparticles with average diameter of 6.6 ± 2.3 nm were observed (Fig. 5(a)). Both gold and silver signals were detected from the nanoparticles, as shown in Figs. 5(b) and 5(c), respectively. It should be noted that signals from silver exhibited shell-like distributions (Fig. 5(b)), whereas gold signals were distributed spherically (Fig. 5(c)). The gold:silver atomic ratio in the nanoparticles was determined to be 88.5:11.5 by EDX analysis. The results show that the formed nanostructures along the bimetallic line structure consist of gold core–silver shell nanoparticles as illustrated in Fig. 5(d).

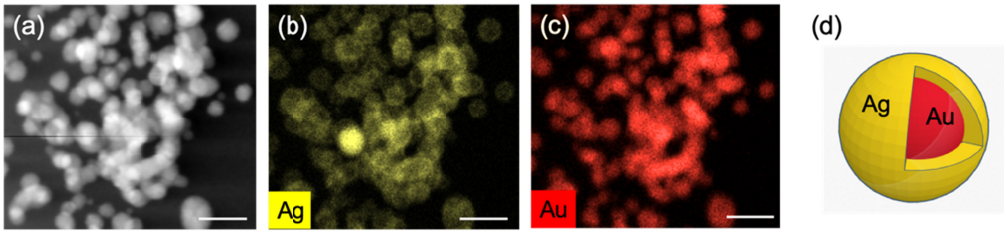


Fig. 5. (a) STEM image and EDX analyses for (b) silver and (c) gold along the fabricated bimetallic line structures. The scale bars represent 20 nm. (d) Schematic illustration of the gold core-silver shell nanoparticle.

Figure 6 shows the typical morphology of the nanoparticle clusters as observed with TEM. The calculated equivalent diameter was 108 nm for the gold nanoparticle cluster (Fig. 6(a)), whereas that for the gold/silver bimetallic nanoparticle cluster was 185 nm (Fig. 6(b)). The gold nanoparticle cluster in Fig. 6(a) has round-edged nanoparticles that can also be seen in the central part of the bimetallic nanoparticle cluster in Fig. 6(b). Angular nanoparticles are seen at the periphery of the cluster in Fig. 6(b), which is a typical structure caused by anisotropic crystal growth for photo-reduced silver particles [41]. The result indicates—in addition to the formation of core–shell bimetallic nanoparticles as shown in Fig. 5—that clusters of nanoparticles are also likely to have a gold core and silver shell–like aggregated structure. The result is related to the absorbance spectra shown in Fig. 4. The slower laser scanning speed for the reduction of silver ions could have formed a thicker silver-nanoparticle layer on a cluster in addition to thickening the shell of individual nanoparticles, resulting in the shift of the absorbance peak.

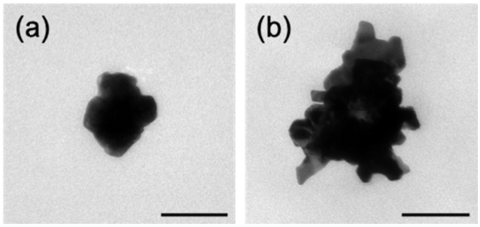


Fig. 6. TEM images of metal nanoparticle clusters formed in the (a) gold grating and in the (b) gold/silver bimetallic structures. The scale bars represent 100 nm.

## 4. Conclusion

We have demonstrated the spatially-targeted fabrication of multi-metal structures coexisting inside the same supporting hydrogel by taking advantages of hydrogel's permeability to fluids. The dissimilar metal microstructures were fabricated site-selectively by scanning femtosecond laser pulses through hydrogel containing metal ions in a stepwise manner. The absorbance peak of the gold/silver bimetallic grid within the hydrogel shifted from those of the gold or silver gratings, which is attributable to the different resonance wavelengths of the nanoparticles. It was shown that the resonant wavelength can be changed by changing laser scanning speed as well as by changing the arrangement of the gratings. STEM and EDX

Optics EXPRESS

analysis revealed that the fabricated bimetallic structure consisted of core–shell nanoparticles. By allowing for site-selective optical properties, the fabrication of dissimilar metal structures within hydrogel is a promising technique for optically driven actuators. Sensing applications, such as devices for glucose and gas measurements, are also candidates for applying the proposed technique that takes advantage of the permeability of hydrogel.

## Funding

MEXT/JSPS KAKENHI Grant Number 18H03551.

## References

1. J. Homola, S. S. Yee, and G. Gauglitz, "Surface plasmon resonance sensors: review," Sens. Actuators B Chem. **54**(1–2), 3–15 (1999).
2. S. E. Skrabalak, J. Chen, L. Au, X. Lu, X. Li, and Y. Xia, "Gold nanocages for biomedical applications," Adv. Mater. **19**(20), 3177–3184 (2007).
3. K. J. Lee, P. D. Nallathamby, L. M. Browning, C. J. Osgood, and X.-H. N. Xu, "*In vivo* imaging of transport and biocompatibility of single silver nanoparticles in early development of zebrafish embryos," ACS Nano **1**(2), 133–143 (2007).
4. Y. Montelongo, J. O. Tenorio-Pearl, C. Williams, S. Zhang, W. I. Milne, and T. D. Wilkinson, "Plasmonic nanoparticle scattering for color holograms," Proc. Natl. Acad. Sci. U.S.A. **111**(35), 12679–12683 (2014).
5. J. Reguera, J. Langer, D. Jiménez de Aberasturi, and L. M. Liz-Marzán, "Anisotropic metal nanoparticles for surface enhanced Raman scattering," Chem. Soc. Rev. **46**(13), 3866–3885 (2017).
6. C. Rehbock, J. Jakobi, L. Gamrad, S. van der Meer, D. Tiedemann, U. Taylor, W. Kues, D. Rath, and S. Barcikowski, "Current state of laser synthesis of metal and alloy nanoparticles as ligand-free reference materials for nano-toxicological assays," Beilstein J. Nanotechnol. **5**, 1523–1541 (2014).
7. A. K. Samal, L. Polavarapu, S. Rodal-Cedeira, L. M. Liz-Marzán, J. Pérez-Juste, and I. Pastoriza-Santos, "Size tunable Au@Ag core-shell nanoparticles: synthesis and surface-enhanced Raman scattering properties," Langmuir **29**(48), 15076–15082 (2013).
8. Q. Han, C. Zhang, W. Gao, Z. Han, T. Liu, C. Li, Z. Wang, E. He, and H. Zheng, "Ag-Au alloy nanoparticles: Synthesis and in situ monitoring SERS of plasmonic catalysis," Sens. Actuators B Chem. **231**, 609–614 (2016).
9. J. Tien, C. M. Nelson, and C. S. Chen, "Fabrication of aligned microstructures with a single elastomeric stamp," Proc. Natl. Acad. Sci. U.S.A. **99**(4), 1758–1762 (2002).
10. D. J. Beesley, J. Semple, L. Krishnan Jagadamma, A. Amassian, M. A. McLachlan, T. D. Anthopoulos, and J. C. deMello, "Sub-15-nm patterning of asymmetric metal electrodes and devices by adhesion lithography," Nat. Commun. **5**(3933), 3933 (2014).
11. J. Semple, D. G. Georgiadou, G. W. Moon, M. Yoon, A. Seitkhan, E. Yengel, S. Rossbauer, F. Bottacchi, M. A. McLachlan, D. D. C. Bradley, and T. D. Anthopoulos, "Large-area plastic nanogap electronics enabled by adhesion lithography," Flexible Electron. **2**(18), 1–10 (2018).
12. S. Maruo, O. Nakamura, and S. Kawata, "Three-dimensional microfabrication with two-photon-absorbed photopolymerization," Opt. Lett. **22**(2), 132–134 (1997).
13. L. Li and J. T. Fourkas, "Multiphoton polymerization," Mater. Today **10**(6), 30–37 (2007).
14. Y.-L. Zhang, Q.-D. Chen, H. Xia, and H.-B. Sun, "Designable 3D nanofabrication by femtosecond laser direct writing," Nano Today **5**(5), 435–448 (2010).
15. M. T. Raimondi, S. M. Eaton, M. M. Nava, M. Laganà, G. Cerullo, and R. Osellame, "Two-photon laser polymerization: from fundamentals to biomedical application in tissue engineering and regenerative medicine," J. Appl. Biomater. Funct. Mater. **10**(1), 55–65 (2012).
16. F. Mayer, S. Richter, J. Westhauser, E. Blasco, C. B. Kowollik, and M. Wegener, "Multimaterial 3D laser microprinting using an integrated microfluidic system," Sci. Adv. **5** (eaau9160), 1–7 (2019).
17. C. N. LaFratta, J. T. Fourkas, T. Baldacchini, and R. A. Farrer, "Multiphoton fabrication," Angew. Chem. Int. Ed. Engl. **46**(33), 6238–6258 (2007).
18. N. Takeyasu, T. Tanaka, and S. Kawata, "Fabrication of 3D metal-polymer microstructures by site-selective metal coating," Appl. Phys., A Mater. Sci. Process. **90**(2), 205–209 (2007).
19. A. Ishikawa, T. Tanaka, and S. Kawata, "Improvement in the reduction of silver ions in aqueous solution using two-photon sensitive dye," Appl. Phys. Lett. **89**(11), 113102 (2006).
20. Y.-Y. Cao, N. Takeyasu, T. Tanaka, X.-M. Duan, and S. Kawata, "3D metallic nanostructure fabrication by surfactant-assisted multiphoton-induced reduction," Small **5**(10), 1144–1148 (2009).
21. S. Tabrizi, Y. Cao, B. P. Cumming, B. Jia, and M. Gu, "Functional optical plasmonic resonators fabricated via highly photosensitive direct laser reduction," Adv. Opt. Mater. **4**(4), 529–533 (2016).
22. T. Tanaka, A. Ishikawa, and S. Kawata, "Two-photon-induced reduction of metal ions for fabricating three-dimensional electrically conductive metallic microstructure," Appl. Phys. Lett. **88**(8), 081107 (2006).
23. S. Maruo and T. Saeki, "Femtosecond laser direct writing of metallic microstructures by photoreduction of silver nitrate in a polymer matrix," Opt. Express **16**(2), 1174–1179 (2008).
24. K. Vora, S. Kang, S. Shukla, and E. Mazur, "Fabrication of disconnected three-dimensional silver nanostructures in a polymer matrix," Appl. Phys. Lett. **100**(6), 063120 (2012).

Optics EXPRESS


25. R. Nakamura, M. Hitomi, K. Kinashi, W. Sakai, and N. Tsutsumi, "Two-photon excitation by femtosecond laser in poly(*N*- vinylpyrrolidone) matrix doped with silver ions," Chem. Phys. Lett. **558**, 62–65 (2013).
26. S. Kang, K. Vora, and E. Mazur, "One-step direct-laser metal writing of sub-100 nm 3D silver nanostructures in a gelatin matrix," Nanotechnology **26**(12), 121001 (2015).
27. J. Qiu, M. Shirai, T. Nakaya, J. Si, X. Jiang, C. Zhu, and K. Hirao, "Space-selective precipitation of metal nanoparticles inside glasses," Appl. Phys. Lett. **81**(16), 3040–3042 (2002).
28. N. N. Nedyalkov, N. E. Stankova, M. E. Koleva, R. Nikov, P. Atanasov, M. Grozeva, E. Iordanova, G. Yankov, L. Aleksandrov, R. Iordanova, and D. Karashanova, "Optical properties modification induced by laser radiation in noble-metal-doped glasses," J. Phys. Conf. Ser. **992**, 012047 (2018).
29. Q. Shi, H. Xia, P. Li, Y.-S. Wang, L. Wang, S.-X. Li, G. Wang, C. Lv, L.-G. Niu, and H.-B. Sun, "Photothermal surface plasmon resonance and interband transition-enhanced nanocomposite hydrogel actuators with hand-like dynamic manipulation," Adv. Opt. Mater. **5**(22), 1700442 (2017).
30. M. Mesch, C. Zhang, P. V. Braun, and H. Giessen, "Functionalized hydrogel on plasmonic nanoantennas for noninvasive glucose sensing," ACS Photonics **2**(4), 475–480 (2015).
31. M. Terakawa, M. L. Torres-Mapa, A. Takami, D. Heinemann, N. N. Nedyalkov, Y. Nakajima, A. Hördt, T. Ripken, and A. Heisterkamp, "Femtosecond laser direct writing of metal microstructure in a stretchable poly(ethylene glycol) diacrylate (PEGDA) hydrogel," Opt. Lett. **41**(7), 1392–1395 (2016).
32. M. Machida, Y. Nakajima, M. L. Torres-Mapa, D. Heinemann, A. Heisterkamp, and M. Terakawa, "Shrinkable silver diffraction grating fabricated inside a hydrogel using 522-nm femtosecond laser," Sci. Rep. **8**(1), 187 (2018).
33. Y. Niidome, A. T. Haine, and T. Niidome, "Anisotropic gold-based nanoparticles: preparation, properties, and applications," Chem. Lett. **45**(5), 488–498 (2016).
34. K. Kyaw, H. Ichimaru, T. Kawagoe, M. Terakawa, Y. Miyazawa, D. Mizoguchi, M. Tsushida, and T. Niidome, "Effects of pulsed laser irradiation on gold-coated silver nanoplates and their antibacterial activity," Nanoscale **9**(41), 16101–16105 (2017).
35. A. Cavallo, M. Madaghiele, U. Masullo, M. G. Lionetto, and A. Sannino, "Photo-crosslinked poly(ethylene glycol) diacrylate (PEGDA) hydrogels from low molecular weight prepolymer: Swelling and permeation studies," J. Appl. Polym. Sci. **134**(2), 44380 (2017).
36. C. J. Orendorff, T. K. Sau, and C. J. Murphy, "Shape-dependent plasmon-resonant gold nanoparticles," Small **2**(5), 636–639 (2006).
37. S. Agnihotri, S. Mukherji, and S. Mukherji, "Size-controlled silver nanoparticles synthesized over the range 5-100 nm using the same protocol and their antibacterial efficacy," RSC. Adv. **4**, 3974–3983 (2014).
38. B. Liedberg, I. Lundström, and E. Stenberg, "Principles of biosensing with an extended coupling matrix and surface plasmon resonance," Sens. Actuators B Chem. **11**(1-3), 63–72 (1993).
39. M. Lau, R. G. Niemann, M. Bartsch, W. O'Neill, and S. Barcikowski, "Near-field-enhanced, off-resonant laser sintering of semiconductor particles for additive manufacturing of dispersed Au-ZnO-micro/nano hybrid structures," Appl. Phys., A Mater. Sci. Process. **114**(4), 1023–1030 (2014).
40. L. Jonušauskas, M. Lau, P. Gruber, B. Gökce, S. Barcikowski, M. Malinauskas, and A. Ovsianikov, "Plasmon assisted 3D microstructuring of gold nanoparticle-doped polymers," Nanotechnology **27**(15), 154001 (2016).
41. Z. Hosseinidoust, M. Basnet, T. G. M. van de Ven, and N. Tufenkji, "One-pot green synthesis of anisotropic silver nanoparticles," Environ. Sci. Nano **3**(6), 1259–1264 (2016).